Development of the high power mercury target and the bubbler installation

Katsuhiro Haga, Hiroyuki Kogawa, Takashi Wakui, Takashi Naoe, Masatoshi Futakawa

Japan Atomic Energy Agency, 2-4 Shirakata Shirane Tokai-mura Ibaraki-ken Japan

E-mail : haga.katsuhiro@jaea.go.jp

Abstract. Cavitation damage of the target vessel wall which is caused by the pressure wave in mercury induced by the pulsed high power proton beam injection is the crucial issue for the development of the high power mercury target. Microbubble injection into mercury is one of the prospective technologies to mitigate the pressure wave. Mercury flow experiments were performed to investigate the bubble flow phenomena in the actual target size of J-PARC. We found that the proper size of microbubbles were distributed around the beam window. Due to the improvement of the target structure, the bubble distribution in mercury was improved by the swirl motion of mercury generated at the bubbler. In the evaluation of the effect of large bubbles to the target wall cooling, large bubbles passing through the high heat load area cause no serious temperature rise of the wall. Based on the study of bubble distribution in the target vessel, the #3 target vessel equipped with swirl type bubblers was developed and installed successfully. In order to improve the target structure further, the double walled window design will be applied to the next target vessel.

1. Introduction

The high-power pulsed spallation neutron source of the Japan Proton Accelerator Research Complex (J-PARC) started its operation in May 2008, and now it is used as one of the most powerful facilities in the world for the research in the most advanced field of material and life science [1)]. However there are some issues to achieve full-power operation at 1MW. The most significant one is the cavitation problem. When the short-pulse high-power proton beam is injected into the mercury target, pressure waves are generated by the abrupt thermal expansion of mercury which may cause cavitation damage to the target vessel wall. Because cavitation damage degrades the structural integrity and seriously decreases the lifetime of the target vessel [2,3)], technologies to mitigate pressure waves have been crucially needed.

Microbubble injection into mercury is one of the prospective technologies to mitigate the pressure wave, and the effect of microbubbles has been investigated experimentally and numerically [4,5,6,7)]. The injected microbubbles are expected to absorb thermal expansion of the mercury at the heat source location, and attenuate the pressure wave during the propagation process [4,5)]. Okita showed by numerical simulations that bubbles with radius less than 100 μm are desirable to mitigate pressure waves effectively [4)]. To realize these effects, several difficulties must be overcome. First of all, microbubbles must be properly distributed in the area of the peak heat load, where is the source location of strong pressure waves. Since liquid mercury has a large density compared with liquid water, microbubbles should be subject to strong buoyancy, and hence controlling the bubble distribution in

flowing mercury may be difficult. The other concern is that essential cooling of the target vessel by the mercury might be degraded by the injected gas. Since the thermal diffusivity of gases is much lower than that of liquid mercury, accumulated gas layers attached to the surface of the vessel walls could significantly decrease the cooling performance.

In this paper, we report the results on a water loop and mercury loop test using a mockup model of the target vessel, performed as one of the studies for a mercury target design with bubbling system. The water loop test was carried out in JAEA. The mercury loop test was carried out under the collaboration with the Oak Ridge National Laboratory (ORNL) using their Target Test Facility (TTF), which is an actual-scale mercury loop constructed for the mercury target development at ORNL. We performed these experiments to investigate the bubble flow phenomena in the actual target size of J-PARC.

We also report the design of the third target equipped with a bubbler in it, and the operational test result. Lastly further improvement of the target structure and the future schedule will be presented.

2. Experimental setup

Figure 1 shows the schematic view of the mockup model of the mercury target. The sizes of the model are 961 mm in length, 545 mm in width, and 220 mm in height. Because the mercury flow field and the bubble rising motion due to buoyancy were considered to be the dominant factors to determine the bubble distribution, the arrangement of the flow vanes and the size of the model were made almost the same as the actual target. The forefront wall of the target vessel, where proton beam is injected, is called the beam window. Because the beam window is very close to the source location of strong pressure waves, it is the most vulnerable place to cavitation damage. Thus, distributing microbubbles around the beam window is the most important point to mitigate pressure waves effectively. The top wall of the mockup model was made of transparent acrylic plates to observe the bubbles rising up to the inner surface of the top wall. The transparent acrylic top wall is 50 mm thick to endure an internal pressure of 1 MPa required by the TTF safety rules. The side walls were made with flat plate to simplify the model structure, while the actual target has rounded side walls. The bubble generator, hereafter called bubbler, was installed at the mercury inlet. A swirl type bubbler was used in this experiment. The performance of the swirl type bubbler was evaluated in a small mercury loop in advance where generated microbubbles from several tens to several hundreds micro meters in radius. Pressure gages were mounted at the inlet and outlet of the bubbler and the outlet of the target vessel.

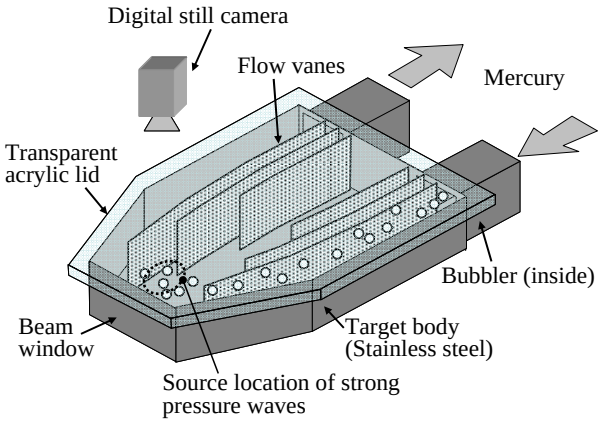

Figure 1. Schematic view of the mockup model

3. Experimental conditions and techniques

The water experiment was carried out at water flow rate of 5 L/s and 10 L/s, and the mercury experiment was carried out at mercury flow rates of 5 L/s and 7.5 L/s while the mercury flow rate of the actual system is 11.4L/s. These flow rates correspond to water velocities of 0.5 m/s, 1 m/s and mercury velocities of 0.5 m/s, 0.75 m/s and 1.14 m/s at the target model inlet, respectively. The maximum flow rate determined based on the pressure loss at the bubbler to maintain its structural integrity because it was made of synthetic resin. The amount of helium supplied to the bubbler was 0.1 % in volume percent of the mercury flow, which was an optimum value for bubbler performance.

The microbubbles were generated and scattered by the swirl type bubbler continuously, hence the bubble distribution at the outlet of the bubbler was assumed to be quasi-homogeneous.

Images of the bubbles on the inner surface of the top wall were taken with a digital still camera which was model D200 of Nicon with a Micro Nikkor lens 105mm and a teleconverter mounted on it. The shutter interval was 0.2 s and the shutter speed was 1/8000 s. An extra light source was used to get proper brightness.

Figure 2 shows the bubble motion schematically. The dimension of the field of view was 33 x 22mm2. B1 and B2 in Fig. 2 (a) are the free bubbles flowing in mercury and appear in the field of view when they reach the top wall in Fig. 2 (b). We wanted to count the number of such free bubbles in the image. On the other hand, B3 and B4 are bubbles clinging to the top wall all the way, whose origins are not clear. After new free bubbles reached the top wall one after another and the number increased in the field of view, a large gas slug passed through the field and most of the small bubbles were cleared as shown in Fig. 2 (c). This was the repeating pattern of bubble behavior in the image. Thus, only the bubbles newly appeared in the image were counted as the valid data to abstract free bubbles like B1 and B2. Because of the obtuse contact angle of mercury on the wall, the bubble size clinging to the wall surface appears larger than that of the free bubble. This effect was taken into consideration to correct the bubble sizes on the image to the free bubble sizes. Because the bubbles with radii up to several hundred micro-meters were of interest, bubbles larger than 1 mm were not counted. Bubbles appearing in the field of view in 1 s which included five sequential images were counted to obtain the bubble size distribution.

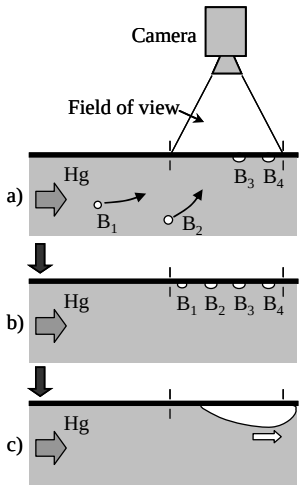

Figure 2. Schematic motion of bubbles appearing on the top wall

4. Bubble size distribution near beam window

4.1. Estimation of bubble size in mercury based on water experiment

Mercury loop experiment is not the easy way to carry out because of the difficulties of handling mercury, and the large scale mercury loop is rare in the world. The water loop experiment is much easy way, and it is ideal that the bubble behaviour in mercury can be estimated based on the data of water experiment. Then, we tried to estimate the bubble size distribution in mercury based on the water experiment.

We assumed that the reachable distance of bubbles from the bubbler becomes the same both for water and mercury if the ratio of the rising velocity of bubbles over the liquid velocity which is expressed by U/V, takes the same value. The rising velocity of bubbles in liquid is the function of the bubble size, and it can be estimated by using the existing studies. When the bubble size in water is fixed, the corresponding rising velocity can be estimated. Then U/V of mercury which has the same value of water is calculated and the corresponding size of bubbles in mercury is calculated from U for mercury.

4.2. Experimental result

Figure 3 shows the experimental results and the converted value of the bubble size distribution in the vicinity of the beam window. The flow rate was 7.5 L/s for mercury, and 5 L/s for water experiment. It can be seen that the bubble sizes were concentrated outstandingly in the range less than 100 μm in radius and only a few bubbles were seen in the larger range.

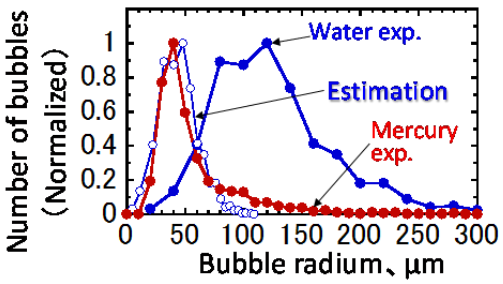

Figure 3. Distribution of bubble radius

In the actual mercury flow, flowing distances and sizes of bubbles will be affected by the flow turbulence and bubble coalescences. These influences will be investigated further in the future. The good findings were that the bubbles observed near the beam window had the ideal size for our purpose to suppress the pressure wave. In the actual mercury target, it is expected that more bubbles will be transported rapidly to the beam window due to the higher mercury flow rate of 11.4 L/s.

In the water experiment, the bubble size distributes from 30 μm to 300 μm in radius, and the converted distribution for mercury agrees well with the experimental result for the mercury experiment. This shows that the ratio U/V is the important factor to estimate the bubble size distribution in liquid.

5. Evaluation of void fraction

Here the void fraction is defined as the volumetric ratio of gas or bubbles in liquid. Figure 4 shows the experimental result of void fraction along the mercury flow channel. Distance from the bubbler of 1.1 m corresponds to the position of the vicinity of the beam window. The volume fraction of the injected gas to the bubbler is 10^{-3}. It can be seen that the void fraction of bubbles is in the order of 10^{-5} both for the mercury flow velocity of 5 m/s and 7.5 m/s in spite of the fact that the injected gas is 10^{-3}. There is a tendency that the distribution of the void fraction becomes flat as the mercury velocity increases. Because these experimental data are measured at the top surface of the flow channel, the void fraction at the bottom is considered to be smaller than the results.

In order to increase the void fraction at the bottom of the flow channel, we carried out the simulation study taking the mercury swirl motion, which is generated at the bubbler, into consideration. Figure 5 shows the results. Here the void fraction of 10^{-4} was assumed at the top surface based on the experimental results. While the void fraction is less than 10^{-6} in the case of no swirl motion, it increased to the order of 10^{-5} and the void fraction distribution became more uniform when the swirl motion was considered. This swirl motion of mercury in the downstream of the bubbler was actually observed in the experiment.

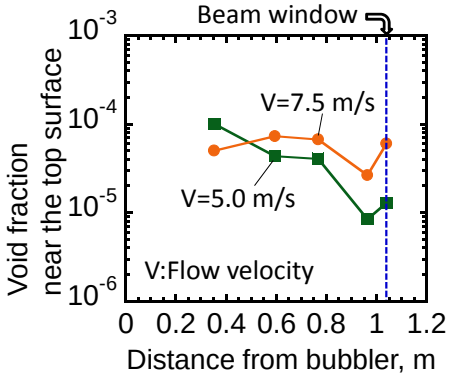

Figure 4. Void fraction along the mercury flow channel

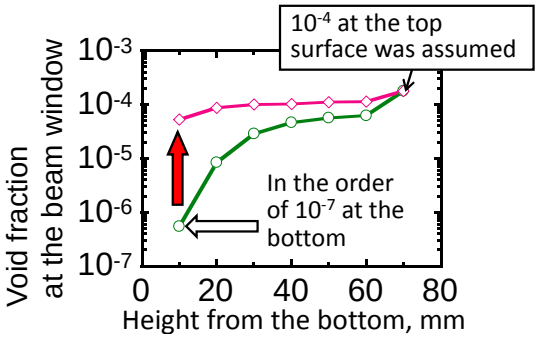

Figure 5. Void fraction in vertical direction at the beam window

6. Effect of large bubble flow to the wall temperature

Large bubbles with radii from several to ten mm, which were formed by the coalescence of injected small bubbles, are strongly affected by the centrifugal force of the flow channel curvature near the beam window. In the experiment, large bubbles passing through the high heat density area, which is 24 W/cm^3, were observed. These bubbles will reduce the wall cooling performance, so the time ratio of no cooling due to the bubble existence at the top wall was evaluated using the image processing of the experimental data, and the time ratio of no cooling was 0.5. On the other hand, the effect of the intermittent bubble flow on the cooling performance of mercury was evaluated. The temperature of the wall was estimated by the 2D model simulation as shown in Figure 6. The heat transfer coefficient at

the central part was fluctuated to simulate the bubbles passing through the area, while that in the other area of the model was set as to cooled by mercury flow. Figure 7 shows the simulation result. At the time ratio of 0.5 which was obtained by the experimental data processing, the estimated temperature rise in the top wall due to the bubble flow was 30 ˚C, which was not so significant.

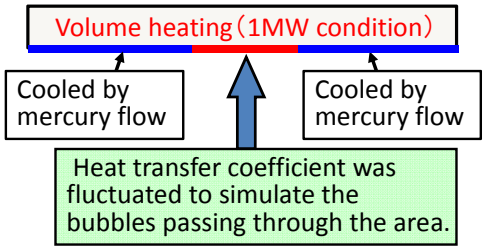

Figure 6. 2D simulation model to evaluate the effect of large bubbles on the top wall cooling

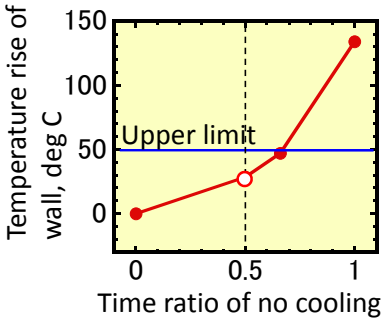

Figure 7. Simulation results of top wall temperature

7. Improvement of #3 target design

On the bases of the experimental results shown above, the structure of the third target vessel was designed. The bubbler was installed to the actual target system for the first time, and the flow channel was designed to place the bubbler near the beam window to improve the bubble distribution at the beam window. In order to compensate for the pressure drop at the bubbler and to adjust the mercury flow distribution in the vessel, the perforated plate was added to the structure. The perforated plate is a plate with array of holes of 4 x 9 of which the center distance is 8 mm. Based on the analytical study, the optimum diameter of holes were decided to be 5 mm. Figure 8 shows the operational test result of the third target after its installation to the target system. The pressure drop of less than 0.2 MPa at the mercury flow rate of 37 m^3/h, which was the design condition of the bubbler, was attained.

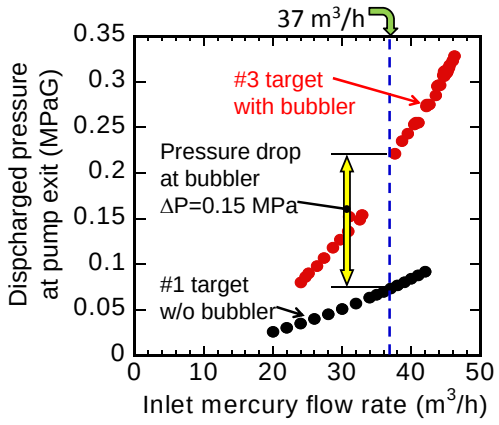

Figure 8. Pressure data of the target system

8. Target design with double walled beam window

The effect of double wall to mitigate the pitting damage was demonstrated in the beam window channel of SNS target where the mercury flow of ca.3 m/s sweeps the surface of the wall, and no obvious pitting damage was observed while the inner surface facing to the bulk mercury flow of low velocity was terribly damaged. This may be due to the high mercury flow rate, of which effect has been investigated in JAEA and SNS, and the narrow flow channel which prevents the cavitation bubble to grow larger.

We are now designing the target vessel with the double walled beam window. In addition to the mitigation effect of pitting damage by the rapid mercury flow, the multiple walls extend the lifetime of the beam window before the pits penetrate two walls. The analytical evaluation for the mercury flow and the flow distribution was carried out, and we could get the prospect that the mercury velocity of ca. 3 m/s can be attained in the mercury channel of double wall. The next target will be equipped with the improved structure.

9. Summary

In the mercury flow experiment, bubbles of proper sizes were distributed at the beam window, and the bubble distribution in mercury was improved by the swirl motion of mercury generated at the bubbler. In the evaluation of the effect of large bubbles to the target wall cooling, large bubbles passing through the high heat load area cause no serious temperature rise of the wall. Based on the study of bubble distribution in the target vessel, the #3 target vessel equipped with swirl type bubblers was developed and installed successfully. In order to improve the target structure further, the double walled window design will be applied to the next target vessel.

Further improvement of the target and the bubbler will be continued.

References

[1] S. Nagamiya, “J-PARC project in japan”, Nuclear Physics A, 774, 895-898 (2006).

[2] M. Futakawa, T. Naoe, C.C. Tsai, H. Kogawa, S. Ishikura, Y. Ikeda, H. Soyama, H. Dta, J. , “Pitting damage by pressure waves in a mercury target “, Nucl. Mater. 343, 70-80 (2005).

[3] M. Futakawa, T. Wakui, H. Kogawa, Y. Ikeda, “ Pressure wave issues in high power mercury target”, Nucl. Instr. and Meth. A 562, 676-679 (2006).

[4] K.Okita, S. Takagi, Y. Matsumoto, “Propagation of Pressure Waves, Caused by a Thermal Shock, in Liquid Metals Containing Gas Bubbles”, J. Fluid Sci. Tech. 3, 116-128 (2008).

[5] M. Futakawa, H. Kogawa, S. Hasegawa, M. Ida, K. Haga, T. Wakui, T. Naoe, N. Tanaka, Y. Matsumoto, Y. Ikeda, “R&D on pressure-wave mitigation technology for pulsed high-power mercury targets”, Proc. of ICANS-XVIII (2007)

[6] M. Ida, T. Naoe, M. Futakawa, “Suppression of cavitation inception by gas bubble injection: A numerical study focusing on bubble-bubble interaction”, Phys. Rev. E 76 (2007) 046309.

[7] T. Naoe, M. Ida, M. Futakawa, “Cavitation damage reduction by microbubble injection“, Nucl. Instr. and Meth. A 586, 382-386 (2008).